Available online at www.sciencedirect.com

SCIENCE DIRECT®

Journal of Organometallic Chemistry 689 (2004) 3335–3349

Journal of Organo metallic Chemistry

www.elsevier.com/locate/jorganchem

Mononuclear and heterodinuclear transition metal complexes of functionalized phosphines. Crystal and molecular structures of $[Mo(CO)_5(RPC_6H_4OCH_2OCH_3\text{-}o)](R = Ph, C_6H_4OCH_2OCH_3\text{-}o)$, $[Ru(Ph_2PC_6H_4O\text{-}o)_3]$, $[Pd(Ph_2PC_6H_4O\text{-}o)_2]$ and $[PdCl(Ph_2PC_6H_4O\text{-}o)(Ph_2PC_6H_4OH\text{-}o)]$

Srinivasan Priya [a], Maravanji S. Balakrishna [a,*], Joel T. Mague [b]

[a] Department of Chemistry, Indian Institute of Technology, Bombay, Mumbai 400 076, India
[b] Department of Chemistry, Tulane University, New Orleans, Louisiana, LA 70118, USA

Received 22 June 2004; accepted 24 July 2004
Available online 28 August 2004

Abstract

Transition metal complexes of phosphine ethers ($Ph_2PC_6H_4OCH_2OCH_3$-*o* and $PhP(C_6H_4OCH_2OCH_3\text{-}o)_2$) and phosphinophenol, $Ph_2PC_6H_4OH$-*o* are described. Phosphine ethers react with Group 6 metal carbonyls to form complexes of the type $[M(CO)_4L_2]$ and $[M(CO)_5L]$ (M = Mo, Cr, W). The reaction of $Ph_2PC_6H_4OCH_2OCH_3$-*o* with $RuCl_3 \cdot 3H_2O$ gave ruthenium(III) complex, $[Ru(Ph_2PC_6H_4O\text{-}o)_3]$ through the elimination of CH_3OCH_2Cl whereas the reaction with $CpRu(PPh_3)_2Cl$ resulted in the formation of $[CpRu(Ph_2PC_6H_4O\text{-}o)PPh_3]$. Treatment of $Ph_2PC_6H_4OCH_2OCH_3$-*o* with rhodium(I) derivatives resulted in the formation of complexes with the phosphine exhibiting both mono- and bidentate modes of coordination involving the phosphorus center and the phenolic oxygen. The reaction of $Ph_2PC_6H_4OCH_2OCH_3$-*o* with $[PdCl_2(COD)]$ led to the isolation of two mononuclear complexes, $[PdCl(Ph_2PC_6H_4O\text{-}o)(Ph_2PC_6H_4OH\text{-}o)]$ cocrystallized with phosphonium salt, $[Ph_2P(CH_2OCH_3)C_6H_4OH\text{-}o]Cl$ and $[Pd(Ph_2PC_6H_4O\text{-}o)_2]$ as confirmed by X-ray diffraction studies. The former shows extensive hydrogen bonding interactions between the complex and the phosphonium salt. The metalloligand, $Cp_2Zr(OC_6H_4PPh_2\text{-}o)_2$ obtained by the reaction of Cp_2ZrCl_2 with $Ph_2PC_6H_4OH$-*o* form heterobimetallic complexes with Mo(0), Re(I) and Ni(0) carbonyl derivatives. The reactions of $Cp_2Zr(OC_6H_4PPh_2\text{-}o)_2$ with metal halides such as $M(COD)Cl_2$(M = Pd, Pt) and $CpRuCl(PPh_3)_2$ afforded metallacycles, $[M(Ph_2PC_6H_4O\text{-}o)_2]$ and $[CpRu(PPh_2C_6H_4OH\text{-}o)(PPh_2C_6H_4O\text{-}o)]$, respectively *via* transmetallation.

Keywords: Functionalized phosphines; Phosphinoethers; Complexes; Metallacycles; Crystal structure

1. Introduction

Phosphines with pendant ether functionalities are of considerable interest, in particular with respect to the development of potential catalysts [1–3] due to the following advantages: (a) Phosphorus(III) atoms can coordinate to a low valent metal center and stabilize it in a lower oxidation state and enhance the chelating possibilities through the ether O-center, (b) The labile M–O coordinate bond in the chelate complex can be readily cleaved when it is required during the catalytic and biological processes. In contrast, the functional groups can effectively bind to metals in their high-valent states to give metallo-ligands with dangling phosphorus(III) centers. These phosphorus centers can bind to low-valent metals to give heterobimetallic complexes without a formal metal–metal bond yet with

---

[*] Corresponding author. Tel.: +91 22 2576 7181; fax: +91 22 2576 7152/2572 3480.
E-mail address: krishna@iitb.ac.in (M.S. Balakrishna).

0022-328X/$ - see front matter © 2004 Elsevier B.V. All rights reserved.
doi:10.1016/j.jorganchem.2004.07.041

two disparate metals in close proximity. Such heterobimetallic complexes could be very effective in activating small organic molecules due to the "cooperative effect" that arises as a consequence of electron sink and reservoir nature of high-valent and the low-valent metals, respectively [4]. As part of our interest [5] and of others [3,6] in phosphines with various functionalities, herein we report the transition metal complexes of phosphine ethers, $Ph_2PC_6H_4OCH_2OCH_3$-*o* (**1**), $PhP(C_6H_4OCH_2OCH_3$-*o*$)_2$ (**2**) and phosphino phenol, $Ph_2PC_6H_4OH$-*o*.

2. Results and discussion

2.1. Phosphine-ethers

The hemilabile phosphine ethers, $Ph_2PC_6H_4OCH_2OCH_3$-*o* (**1**) and $PhP(C_6H_4OCH_2OCH_3$-*o*$)_2$ (**2**) were synthesized from methoxymethylphenyl ether and $Ph_2PCl/PhPCl_2$ following the literature [7] procedures. When $[M(CO)_4L_2]$ (L_2 = (piperidine)$_2$, NBD or COD) was treated with ligands **1** and **2**, tetracarbonyl complexes of the type, $[M(CO)_4L_2]$ (**3**–**7**) (M = Cr, Mo or W, L = **1** or **2**) were obtained in good yield. The IR spectra of the chromium complexes **3** and **4** show single band in the carbonyl region indicating the formation of *trans*-isomers. The molybdenum and tungsten complexes **5**–**7** each show four strong absorptions in the carbonyl region and so are *cis*-isomers. The ^{31}P NMR chemical shifts (see Section 4) of disubsituted tetracarbonyl complexes, **3**–**7** are more shielded as moved from chromium to tungsten down the group. Reactions of **1** and **2** with $Mo(CO)_6$ in *equimolar* ratio, afforded monosubstituted complexes, $[Mo(CO)_5(PPh_2C_6H_4OCH_2OCH_3$-*o*$)]$ (**8**) and $[Mo(CO)_5\{PPh(C_6H_4OCH_2OCH_3$-*o*$)_2\}]$ (**9**), respectively. The ^{31}P NMR spectra of **8** and **9** show single resonances at 29.5 and 22.6 ppm with the coordination shifts of 45.5 and 49.0 ppm, respectively. The ^1H NMR spectrum of complex **8**, shows a single resonance due to the methylene protons whereas the same in complex **9** appears as an AB quartet indicating their non-equivalence. The IR spectra of **8** and **9** show three bands in the carbonyl region as expected. The structures of complexes **8** and **9** have been established by single crystal X-ray diffraction studies.

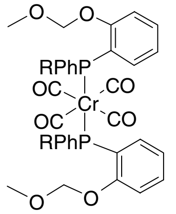

3 R = Ph
4 R = $C_6H_4OCH_2OCH_3$

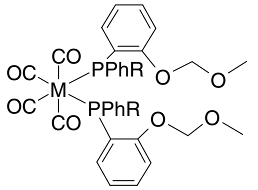

5 M = Mo, R = Ph
6 M = W, R = Ph
7 M = W, R = $C_6H_4OCH_2OCH_3$

Perspective views of complexes **8** and **9** are shown in Fig. 1 while crystallographic data, selected bond distances and bond angles are given in Tables 1 and 2. The crystal structure of **9** reveals the presence of two independent molecules in the asymmetric unit, which differ somewhat in the bond distances and bond angles involving the metal center. The structures of **8** and **9** show octahedral environment around molybdenum centers with *trans* angles in the range of 174.7–175.5° (for complex **8**) and 171.0–175.1° (for complex **9**). The *cis* angles vary in the range of 85.7–93.0° (for complex **8**) and 83.7–97.3° (for complex **9**). The Mo–P bond distances in **8** and **9** are 2.570(1) Å and 2.572(2), 2.578(2) Å, respectively. The Mo–C bond *trans* to the Mo–P bond (av. 1.985 Å) is slightly shorter than the other Mo–C bond distances (av. 2.044 Å) in both the complexes **8** and **9** as expected.

When ligand **1** was treated with $RuCl_3 \cdot 3H_2O$ under reflux conditions, a neutral ruthenium(III) metallacycle, $[Ru(Ph_2PC_6H_4O$-*o*$)_3]$ (**10**) was obtained in good yield. The ether linkage is cleaved during complexation leading to the formation of the phenolate ion, presumably with the elimination of methoxymethyl chloride. The phenolate oxygens bind to the ruthenium center forming three five-membered metallacycles. In contrast, phosphine-ether ligands of the type $R_2PCH_2CH_2OMe$-*o*, $Ph_2PC_6H_4OMe$-*o* when reacted with $RuCl_3{\cdot}3H_2O$, form exclusively bischelate complexes, *trans*-$[RuCl_2$ $(R_2PCH_2CH_2OMe$-*o*$)_2]$ and $[RuCl_2(Ph_2PC_6H_4OMe$-*o*$)_2]$, respectively [2]. Thus, the cleavage could be presumably due to the presence of additional OCH_3 group and which facilitates the elimination of methoxymethyl chloride (**caution:** Methoxymethyl chloride is highly toxic and the reaction has to be performed in a very efficient fume hood). The ^{31}P NMR spectrum of **10** shows a broad peak around 49 ppm owing to its paramagnetic nature. However, structure of complex **10** was confirmed by single crystal X-ray diffraction study. The perspective view of molecule **10** is shown in Fig. 2. The crystallographic data, selected bond distances and bond angles are listed in Tables 1 and 3, respectively. The core RuO3P3 has the three phosphorus and three oxygen centers disposed in a *meridional* arrangement, consequently pairs of donors are mutually *trans* to each other, O(1)/O(2) and P(2)/P(3), whereas P(1) is *trans* to O(3). The Ru–P(1) and Ru–P(2) bond distances are the same (2.347(1) Å) whereas the Ru–P(3) bond which is *trans* to Ru–P(2) is longer with a bond distance of 2.374 Å. Similarly, the bond distances of Ru–O(1)=Ru–O(3) = 2.043(2) Å are longer than the Ru–O(2) (2.006(2) Å) bond distance which is *trans* to Ru–O(1) bond.

The reaction of **1** with $CpRuCl(PPh_3)_2$ in equimolar ratio gave $CpRu(PPh_3)(PPh_2C_6H_4O$-*o*$)$ (**11**) in 42% yield. The ether linkage is cleaved during complexation

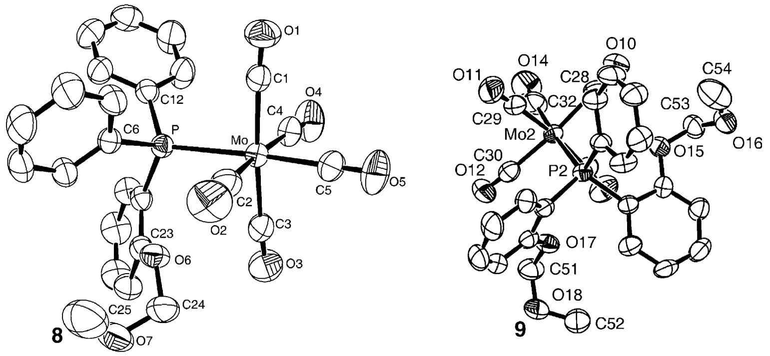

Fig. 1. ORTEP plot of [$Mo(CO)_5(PPh_2C_6H_4OCH_2OCH_3$-*o*)] (**8**) and [$Mo(CO)_5\{PPh(C_6H_4OCH_2OCH_3$-*o*$)_2\}$] (**9**) with thermal ellipsoids are drawn at 50% probability level. Hydrogen atoms are omitted for clarity.

Table 1
Crystallographic data for complexes **8**, **9**, **10**, **16** and **17**

	Complex **8**	Complex **9**	Complex **10**	Complexes **16** and **18**	Complex **17**
Empirical formula	$C_{25}H_{19}MoO_7P$	$C_{27}H_{23}MoO_9P$	$C_{54}H_{42}O_3P_3Ru \cdot CH_2Cl_2$	$C_{36}H_{29}ClO_2P_2Pd \cdot C_{20}H_{20}O_2PCl$	$C_{37.5}H_{31}O_2P_2PdCl_3$
Formula weight	558.31	618.36	1017.78	1056.18	788.31
Crystal system	Monoclinic	Triclinic	Monoclinic	Triclinic	Triclinic
Space group	*P2₁/n* (No. 14)	$P\bar{1}$ (No. 2)	*P2₁/c* (No. 14)	$P\bar{1}$ (No. 2)	$P\bar{1}$ (No. 2)
a	14.9920(9)	9.0561(3)	18.468(3)	11.2638(6)	11.372(2)
b	11.3395(5)	16.6920(8)	13.295(2)	13.4451(7)	11.829(2)
c	15.6674(8)	19.1080(9)	18.867(3)	17.713(1)	14.393(3)
α	90	99.074(4)	90	89.822(1)	89.891(3)
β	108.093(6)	103.669(4)	91.394(2)	78.018(1)	73.388(3)
γ	90	86.875(4)	90	71.691(1)	89.717(4)
V	2531.8(2)	2771.2(2)	4631.1(3)	2485.6(2)	1855.3(6)
Z	4	4	4	2	1
$D_{(calc.)}$	1.465	1.482	1.460	1.411	1.411
λ (Mo Kα)[a] Å	0.71073	0.71073	0.71073	0.71073	0.71073
μ (Mo Kα) (mm)	0.6	0.6	0.6	0.6	0.8
Temperature (K)	293	293	100	100	100
θ min–max (°)	1.6–25.1	1.5–25.1	1.1–28.3	1.6–28.3	1.5–23.3
R[b]	0.0276	0.0470	0.0590	0.0432	0.0723
wR[c]	0.0812	0.1359	0.1404	0.0994	0.2108
a, *b*	0.03676, 0.6313	0.0163, 0.9343	0.0566, 10.3774	0.0480, –	0.1185, –

$w = 1/[\sigma^2(F_o^2) + (aP)^2 + bP]$; $P = 1/3[F_o^2 + 2F_c^2]$.

[a] Graphite monochromated.

[b] $R = \sum|F_o - F_c|/\sum|F_o|$.

[c] $R_w = \left[\sum w(F_o^2 - F_c^2)\Big/\sum w(F_o^2)^2\right]^{1/2}$.

leading to the formation of the phenolate ion, presumably with the elimination of methoxymethyl chloride. The phenolate oxygen binds to the ruthenium center forming a five-membered metallacycle. In a similar way, $Ph_2PC_6H_3(2,6\text{-}OCH_3)_2$ reacted with [(η^6-*p*-cymene)$RuCl_2]_2$ to give [(η^6-*p*-cymene)RuCl{PPh(2,6-MeO)$_2$-C_6H_3(2-O-6-MeOC_6H_3)}] presumably through the elimination of one of the methyl group as CH_3Cl to form a five-membered metallacycle [8]. The same compound is also obtained directly from $Ph_2PC_6H_4OH$-*o*. ^{31}P NMR spectrum of **11** exhibits two doublets at 57.5 and 44.2 ppm with a $^2J_{PRuP}$ coupling of 35.1 Hz. Further support for the formation of **11** comes from its mass spectral data and micro analytical data.

The reaction of **1** with $[Rh(CO)_2Cl]_2$ resulted in the formation of a neutral chelate complex, [Rh(CO)Cl($PPh_2C_6H_4OCH_2OCH_3$-*o*)] (**12**) in good yield. The IR spectrum of **12** shows ν_{CO} at 1956 cm^{-1} and the ^1H NMR spectrum shows shift in the resonances for the CH_2 and CH_3 protons as compared to the free ligand implying the binding of the oxygen to the metal center. The ^{31}P NMR spectrum of **12** shows a doublet at 59.5 ppm with a $^1J_{PRh}$ coupling of 173.8 Hz.

The reaction of **1** with $[Rh(COD)Cl]_2$ gave a mixture of two complexes, [Rh(COD)($PPh_2C_6H_4OCH_2OCH_3$-*o*)Cl] (**13**) and [Rh(COD)(μ-$PPh_2C_6H_4OCH_2OCH_3$-*o*)]$_2Cl_2$ (**14**) in 3:1 ratio as indicated by the ^{31}P NMR spectroscopic data. The ^{31}P NMR spectrum of the

Table 2
Selected bond distances (Å) and bond angles (°) for compounds **8** and **9**

Compound **8**		Compound **9**	
Bond distances (Å)			
Mo–P	2.570(1)	Mo(1)–P(1)	2.575(2)
Mo–C(2)	2.059(3)	Mo(1)–C(2)	2.032(7)
Mo–C(3)	2.049(3)	Mo(1)–C(4)	2.044(7)
Mo–C(5)	1.990(3)	P(1)–C(6)	2.568(2)
P–C(12)	1.842(3)	P(1)–C(18)	2.016(9)
O(1)–C(1)	1.134(4)	Mo(2)–P(2)	2.568(2)
O(3)–C(3)	1.124(4)	P(2)–C(33)	1.844(7)
Mo–C(1)	2.033(3)	Mo(1)–C(1)	2.039(7)
Mo–C(4)	2.031(3)	Mo(1)–C(3)	2.052(7)
P–C(6)	1.837(3)	Mo(1)–C(5)	1.989(7)
P–C(18)	1.836(3)	P(1)–C(12)	2.042(7)
O(2)–C(2)	1.130(4)	P(2)–C(39)	1.848(7)
O(4)–C(4)	1.141(4)	P(2)–C(45)	1.838(7)
O(5)–C(5)	1.142(4)		
Bond angles (°)			
P–Mo–C(1)	92.0(1)	P(1)–Mo(1)–C(1)	97.3(2)
P–Mo–C(3)	91.2(1)	P(1)–Mo(1)–C(3)	89.2(2)
P–Mo–C(5)	174.7(1)	P(1)–Mo(1)–C(5)	175.1(2)
Mo–P–C(12)	118.5(1)	Mo(1)–P(1)–C(6)	119.6(2)
C(6)–P–C(12)	100.7(1)	Mo(1)–P(1)–C(18)	116.0(2)
C(12)–P–C(18)	102.5(1)	P(1)–Mo(1)–C(2)	90.5(2)
P–Mo–C(2)	86.7(1)	P(1)–Mo(1)–C(4)	88.3(2)
P–Mo–C(4)	97.7(1)	Mo(1)–P(1)–C(12)	112.1(2)
C(1)–Mo–C(2)	91.3(1)	C(6)–P(1)–C(12)	105.3(3)
Mo–P–C(6)	115.2(1)	C(12)–P(1)–C(18)	101.4(3)
Mo–P–C(18)	114.5(1)		
C(6)–P–C(18)	103.2(1)		

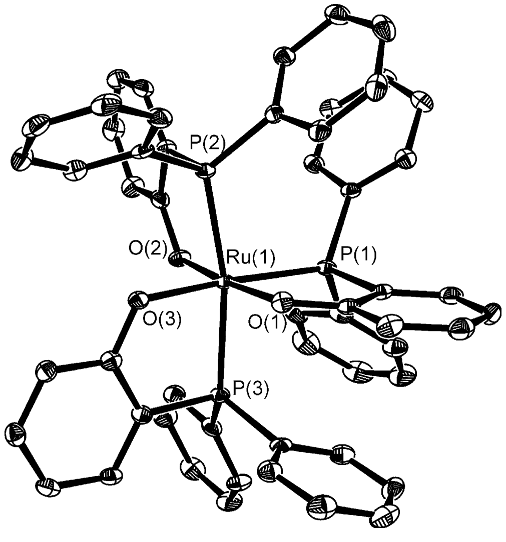

Fig. 2. ORTEP plot of [Ru(Ph$_2$PC$_6$H$_4$O-*o*)$_3$] (**10**). Ellipsoids are drawn at the 50% probability level. Hydrogen atoms are omitted for clarity.

reaction mixture shows two doublets at 23.0 and 48.4 ppm, respectively for **13** and **14** with $^1J_{\mathrm{PRh}}$ couplings of 149.6 and 141.9 Hz. The ^{1}H NMR spectrum also reveals the presence of two complexes in the reaction mixture. Two sets of chemical shifts were observed for the CH$_2$ and CH$_3$ protons in a 3:1 ratio with one set of chemical shifts essentially in the same position that of ligand (due to complex **13**) whereas the other set shows chemical shifts with considerable shielding (due to complex **14**) indicating the coordination of the phenolic oxygen to the metal center. However, after crystallization, complex **13** is obtained exclusively and attempts to isolate the cationic complex **14** have been unsuccessful. The cationic complex, [Rh(COD)(PPh$_2$C$_6$H$_4$O-CH$_2$OCH$_3$-*o*)]BF$_4$ (**15**) was obtained in a separate reaction of **1** with [Rh(COD)Cl]$_2$ in presence of AgBF$_4$. The ^{31}P NMR spectrum of **15** exhibits a doublet at 34.0 ppm with a $^1J_{\mathrm{RhP}}$ coupling of 159.2 Hz. The coordination chemical shift is 60.4 ppm (see Scheme 1).

The reaction of **1** with [Pd(COD)Cl$_2$] in 2:1 molar ratio leads to the formation of a mixture of products as evident from the ^{31}P NMR spectroscopic data. Fractional crystallization of the crude product using a CH$_2$Cl$_2$–diethylether mixture (see Section 4) led to the isolation of three different products **16**–**18** which are characterized by micro analytical data, mass, IR, and NMR spectroscopic data. Formation of complexes, [PdCl(PPh$_2$C$_6$H$_4$O-*o*) (PPh$_2$C$_6$H$_4$OH-*o*)] (**16**) and [Pd (PPh$_2$C$_6$H$_4$O-*o*)$_2$] (**17**) involves the cleavage of a C–O (ether linkage) bond of the ligand, which forms the phenolate ion, presumably with the elimination of methoxymethylchloride as observed in the case of ruthenium complexes **10** and **11**. Similar reaction of Pd(COD)Cl$_2$ with analogous ligand, PPh$_2$C$_6$H$_4$OCH$_3$ affords the simple chelate complex, PdCl$_2$(PPh$_2$C$_6$H$_4$OCH$_3$-*o*)$_2$ [2,9]. In complex **16**, one of the ligands forms a five-membered metallacycle whereas the other binds only through the phosphorus center and the phenolic oxygen is protonated. Complex **17** is consists of two five-membered metallacycles (Scheme 2). Along with these two complexes, the phosphonium salt, [Ph$_2$P(CH$_2$OCH$_3$)-C$_6$H$_4$OH-*o*]Cl (**18**) is also formed, which is co-crystallized with **16**. The formation of **18** may be attributed to the quaternization of the phosphorus(III) center in **1** by CH$_3$OCH$_2$Cl which was eliminated during complexation. Such phosphonium salt formation was not observed in the deprotection reactions of ligands **1** and **2** with anhydrous HCl. The ^{31}P NMR spectrum of **16** shows two doublets at 47.2 and 20.8 ppm with a $^2J_{\mathrm{PP}}$ coupling of 12.3 Hz indicating that one of the ligand binds to the metal in a monodentate fashion whereas the other forms a metallacycle. The ^{31}P chemical shift due to the phosphonium salt, [Ph$_2$P(CH$_2$OCH$_3$)-C$_6$H$_4$OH-*o*]Cl (**18**) appears as a singlet at 16.1 ppm. Complex **17** shows a single resonance at 43.7 ppm in its ^{31}P NMR spectrum indicating the equivalent nature of both the phosphorus centers.

The structure of complex **16** co-crystallized with **18** was established by single crystal X-ray diffraction studies. The structures are shown in Fig. 3 and crystallo-

Table 3
Selected bond lengths (Å) and bond angles (°) for **10**

Bond distances (Å)			
Ru(1)–P(1)	2.347(1)	Ru(1)–P(2)	2.347(1)
Ru(1)–P(3)	2.374(1)	Ru(1)–O(1)	2.043(2)
Ru(1)–O(2)	2.006(2)	Ru(1)–O(3)	2.043(2)
P(1)–C(1)	1.799(3)	P(2)–C(19)	1.809(4)
P(3)–C(37)	1.813(4)		
Bond angles (°)			
P(1)–Ru(1)–P(2)	97.47(3)	P(1)–Ru(1)–P(3)	95.39(3)
P(1)–Ru(1)–O(1)	81.1(1)	P(1)–Ru(1)–O(2)	93.5(1)
P(1)–Ru(1)–O(3)	172.1(1)	P(2)–Ru(1)–P(3)	167.13(3)
P(2)–Ru(1)–O(1)	95.0(1)	P(2)–Ru(1)–O(2)	83.6(1)
P(2)–Ru(1)–O(3)	84.9(1)	P(3)–Ru(1)–O(1)	87.5(1)
P(3)–Ru(1)–O(2)	95.2(1)	P(3)–Ru(1)–O(3)	82.5(1)
O(1)–Ru(1)–O(2)	174.2(1)	O(1)–Ru(1)–O(3)	91.2(1)
O(2)–Ru(1)–O(3)	94.3(1)		

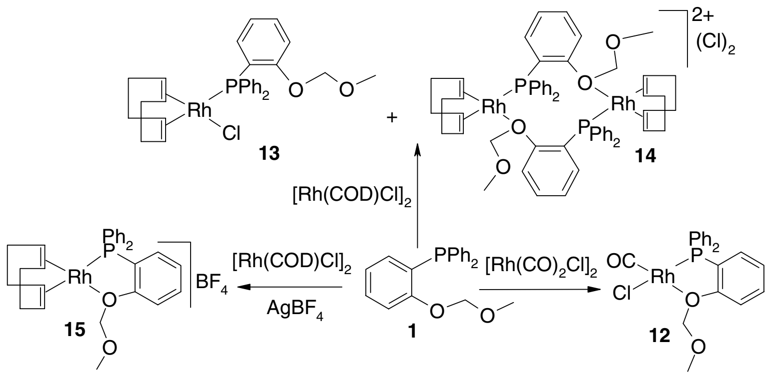

Scheme 1.

graphic data, selected bond distances and bond angles are given in Tables 1 and 4.

In complex **16**, palladium is in a distorted square planar environment with two phosphorus centers in mutually *cis* dispositions. One of the ligands binds in monodentate fashion keeping the OH group intact, whereas the other ligand forms a five-membered metallacycle. The *cis* and *trans* angles are: 100.51(3)° [P(1)–Pd–P(2)], 89.3(2)° [O(1)–Pd–Cl(1)] 173.49(3)° and [Cl(1)–Pd–P(1)], 174.18(6)° [P(2)–Pd–O(1)], respectively. The Pd–P(1) and Pd–P(2) bond distances are 2.241(1) and 2.251(1) Å, respectively. The P(1)–Pd–O(1) angle of 84.88(6)° is also comparable with the same in analogous five-membered metallacycles [10]. The chloride ion in the phosphonium salt is held by five intermolecular hydrogen bonding interactions of which two are the O–H...Cl type and the remaining three are of the C–H...Cl type. This molecule also exhibits one intramolecular and one intermolecular C–H...O type hydrogen bonding interaction. The lattice structure is shown in Fig. 4, where the complex **16** and the phosphonium ion **18** are placed alternately and are linked by Cl^- ions. The different hydrogen bonding parameters are summarized in Table 5.

The structure of bischelate complex **17** was also established by single crystal X-ray diffraction studies. The perspective view of molecule **17** is shown in Fig. 5 and crystallographic data, selected bond distances and bond angles are given in Tables 1 and 6. In complex **17**, palladium is in a distorted square planar environment with two phosphorus centers in mutually *cis* dispositions. The *trans* angles are: P(1)–Pd–O(2) = 173.1(2) and P(2)–Pd–O(1) = 172.9(2)° and the *cis* angles varies from 85.0(2)° to 101.8(1)°.

The reaction of **1** with [Pd(COD)Cl_2] in the presence of two moles of $AgBF_4$ resulted in the formation of ionic complex, $[Pd(PPh_2C_6H_4OCH_2OCH_3\text{-}o)_2](BF_4)_2$ (**19**) as shown in Scheme 2. The ^{31}P NMR spectrum of **19** shows a single resonance at 45.4 ppm.

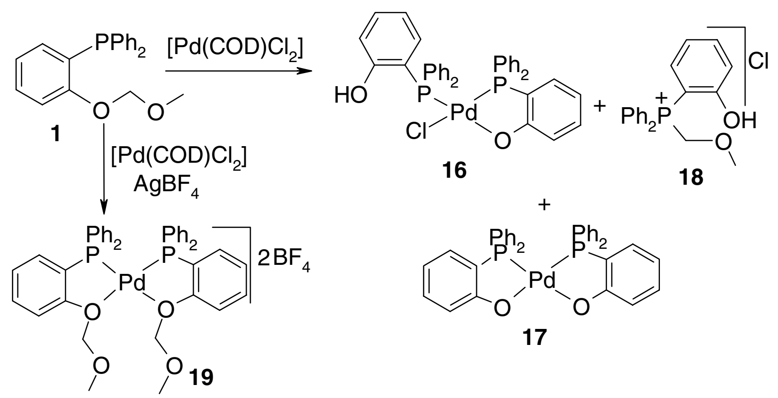

Scheme 2.

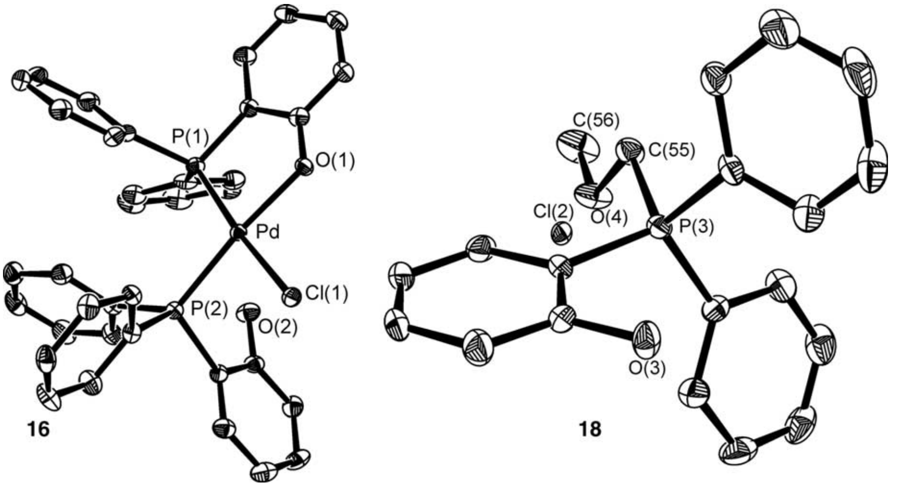

Fig. 3. ORTEP plot of [PdCl($PPh_2C_6H_4O$)($PPh_2C_6H_4OH$-*o*)] (**16**) co-crystallized with [$Ph_2P(CH_2OCH_3)C_6H_4OH$-*o*]Cl (**18**). Ellipsoids are drawn at the 50% probability level. Hydrogen atoms are omitted for clarity.

Table 4
Selected bond distances (Å) and bond angles (°) for **16** and **18**

Bond distances (Å)			
Pd–Cl(1)	2.360(1)	Pd–P(1)	2.241(1)
Pd–P(2)	2.251(2)	Pd–O(1)	2.059(2)
P(23)–C(55)	1.817(3)	P(3)–C(37)	1.781(3)
P(3)–C(43)	1.773(4)	P(3)–C(49)	1.790(3)
Bond angles (°)			
Cl(1)–Pd–P(1)	173.50(3)	Cl(1)–Pd–P(2)	85.40(3)
Cl(1)–Pd–O(1)	89.3(2)	P(1)–Pd–P(2)	100.51(3)
O(1)–Pd–P(1)	84.9(2)	O(1)–Pd–P(2)	174.2(1)
C(37)–P(3)–C(55)	107.2(2)	C(37)–P(3)–C(43)	111.1(1)
C(37)–P(3)–C(49)	114.4(1)	C(49)–P(3)–C(55)	106.1(1)
C(43)–P(3)–C(49)	109.4 (2)	C(43)–P(3)–C(55)	108.5(2)

The reaction of $PhP(C_6H_4OCH_2CH_3\text{-}o)_2$ (**2**) with [Pd(COD)Cl_2] affords [Pd{PPh($C_6H_4OCH_2OCH_3$-*o*)$_2$}$_2Cl_2$] (**20**) in good yield (Scheme 3). The ^{31}P NMR spectrum of **20** shows a single resonance at 14.3 ppm. The formation of **20** is further confirmed by its ^1H NMR spectroscopic data. The reactions of ligands **1** and **2** with [Pt(COD)I_2] in 2:1 molar ratio gave *cis*-[Pt($PPh_2C_6H_4OCH_2OCH_3$-*o*)$_2I_2$] (**21**) and *cis*-[Pt{PPh-($C_6H_4OCH_2OCH_3$-*o*)$_2$}$_2I_2$] (**22**), respectively in good yields. The ^{31}P NMR spectra of **21** and **22** show single resonances at 5.6 and 1.7 ppm with $^1J_{PtP}$ coupling of 2565 and 2611 Hz, respectively. The ^1H NMR spectral data supports the monodentate nature of the ligand whereas the large $^1J_{PtP}$ coupling supports the *cis* geometry around the metal center.

The ^1H and ^{31}P NMR spectral data for compounds **3**–**22** are given in Table 7.

2.2. Phosphinophenol

The reaction of **1** with anhydrous HCl regenerates hydroxy functionality to give phosphinophenol, $Ph_2PC_6H_4OH$-*o* [7].

The reaction of $Ph_2PC_6H_4OH$-*o* with Cp_2ZrCl_2 in the presence of imidazole in dichloromethane gives the metalloligand, $Cp_2Zr(OC_6H_4PPh_2\text{-}o)_2$ (**23**) (Eq. 1).

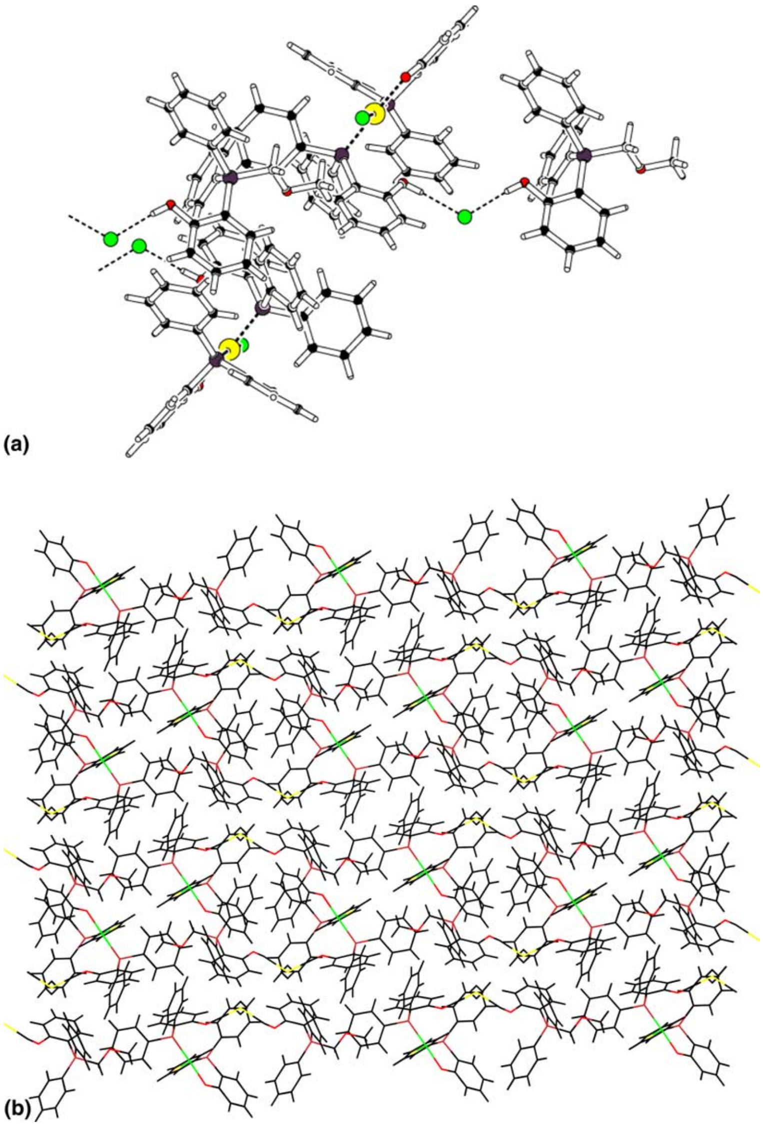

Fig. 4. (a) PLATON diagram of **16** and **18** showing O–H..Cl type intermolecular hydrogen bonding interactions. (b) The lattice structure showing alternate arrangement of complex **16** and phosphonium salt **18** linked by hydrogen bonding.

Table 5
Different hydrogen bonding interactions present in **16** and **18**

D–H. . .A	$d_{\text{H..A}}$ (Å)	$d_{\text{D. . .A}}$ (Å)	D–H–A (°)
O(2)–H(2). . .Cl(2)	2.1525	2.992(20)	178.99
O(3)–H(3). . .Cl(2)	2.0887	2.915(2)	167.99
C(21)–H(21)..Cl(2)	2.8048	3.513(3)	132.11
C(38)–H(38)..O(4)	2.4293	3.117(4)	128.03
C(40)–H(40). . .Cl(2)	2.7193	3.627(3)	160.07
C(45)–H(45). . .Cl(2)	2.7371	3.592(4)	150.11
C(50)–H(50). . .O(1)	2.3131	3.219(4)	159.29

Even though this compound was prepared by Miquel et al. [11] in 1995 to date, only one heterobimetallic complex, [$Cp_2Zr(OC_6H_4PPh_2$-*o*$)_2Rh(CO)Cl$] is reported [11].

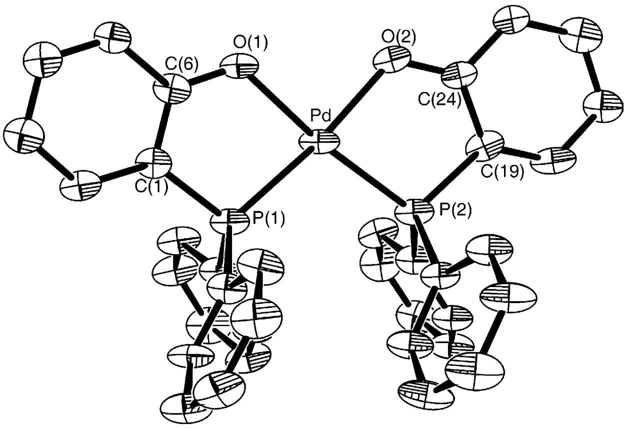

Fig. 5. ORTEP plot of [Pd($PPh_2C_6H_4O$-*o*$)_2$] (**17**). Ellipsoids are drawn at the 50% probability level. Hydrogen atoms are omitted for clarity.

Table 6
Selected bond distances (Å) and bond angles (°) for **17**

Bond distances (Å)			
Pd–P(1)	2.229(3)	Pd–O(1)	2.035(6)
Pd–P(2)	2.224(3)	Pd–O(2)	2.035(6)
Bond angles (°)			
P(1)–Pd–P(2)	101.8(1)	P(1)–Pd–O(1)	85.2(2)
P(1)–Pd–O(2)	173.1(2)	P(2)–Pd–O(1)	172.9(2)
P(2)–Pd–O(2)	85.0(2)	O(1)–Pd–O(2)	88.1(3)

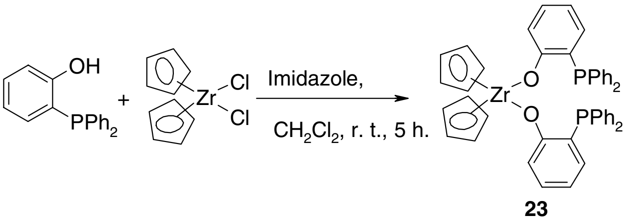

(1)

The reaction of metalloligand **23** with equimolar quantity of $Mo(CO)_6$ in benzene under reflux condition afforded $[(OC)_4Mo(\mu\text{-}PPh_2C_6H_4O\text{-}o)_2ZrCp_2]$ (**24**) as shown in Scheme 4. The ^{31}P NMR spectrum of product shows a single resonance at 39.5 ppm indicating both the phosphorus atoms are equivalent. The IR spectrum shows four ν_{CO} bands indicating the presence of four carbonyl groups on the molybdenum center with C_{2v} symmetry.

The reaction of *fac*-$[Re(CO)_3(CH_3CN)_2Br]$ with **23** in equimolar ratio afforded $[Br(OC)_3Re(\mu\text{-}PPh_2C_6H_4O\text{-}o)_2ZrCp_2]$ (**25**) as shown in Scheme 4. The ^{31}P NMR spectrum of **25** shows doublet of doublets at 9.6 and 26.6 ppm with a $^2J_{PReP}$ coupling of 29.7 Hz, which indicates that the arrangement of three CO ligands is *meridional*. The ^1H NMR spectrum of the compound **25** shows the peak corresponding to cyclopentadienyl protons at 6.37 ppm which are considerably deshielded as compared to the same in metalloligand **23**. IR spectrum of **25** shows three bands in the carbonyl region supporting the *meridional* arrangement.

The reaction of metalloligand **23** with $Ni(CO)_2(PPh_3)_2$ in CH_2Cl_2 at room temperature yielded $[(OC)_2Ni(\mu\text{-}PPh_2C_6H_4O\text{-}o)_2ZrCp_2]$ (**26**). The ^{31}P NMR spectrum of **26** shows a single resonance at 34.3 ppm. IR spectrum of **26** (ν_{CO}: 2004 vs and 1948 vs cm^{-1}) shows the shift of ν_{CO} towards higher wave number when compared to the metal precursor, $Ni(CO)_2(PPh_3)_2$ (ν_{CO}: 1999 s and 1943 vs cm^{-1}). Further evidence for the structural composition of complexes **24**–**26** comes from their mass spectral data.

The reactions of metalloligand, $Cp_2Zr(OC_6H_4PPh_2\text{-}o)_2$ with $M(COD)Cl_2$ (M = Pd, Pt) in CH_2Cl_2 resulted in the formation of chelate complexes $[M(OC_6H_4PPh_2\text{-}o)_2]$ (M = Pd, **17**; Pt, **27**), instead of the anticipated heterobimetallics as shown in Scheme 5. The formation of **17** and **27** could be due to the transmetallation of metalloligand **23** through the elimination of Cp_2ZrCl_2. The ^{31}P and ^1H NMR and mass spectral data supports the formation of **17** and **27**. The ^{31}P NMR spectrum of **27** shows a singlet at 19.0 ppm with $^1J_{PtP}$ coupling of 3540 Hz. The complexes **17** and **27** are reported in the literature by the direct reaction of *o*-diphenylphosphino phenol, $Ph_2PC_6H_4OH\text{-}o$ with corresponding metal derivatives [7a,12].

Upon the reaction of $[CpRuCl(PPh_3)_2]$ with **23** in toluene under reflux conditions, bright orange crystalline product $[CpRu(OC_6H_4PPh_2\text{-}o)(PPh_2C_6H_4OH\text{-}o)]$ (**28**) was isolated. The formation of **28** may be due to the presence of trace amount of moisture, which hydrolyses **23** followed by the protonation of phenolic oxygen. The ^{31}P NMR spectrum of **28** shows doublet of doublets at 63.9 and 45.2 ppm with a $^2J_{PRuP}$ coupling of 37.8 Hz. Further support for the formation of the complex **28** comes from its ^1H NMR spectrum, micro analytical and mass spectral data.

3. Summary

We have demonstrated the versatility of phosphines containing ether functionality which readily form complexes with various transition metal organometallic derivatives. These ligands exhibit both monodentate and bidentate modes of coordination. Group 6 metal carbonyls and Pt(II) derivatives form complexes with free ethereal oxygen ends, whereas Rh(I) derivatives form both chelate and monodentate complexes. Ether

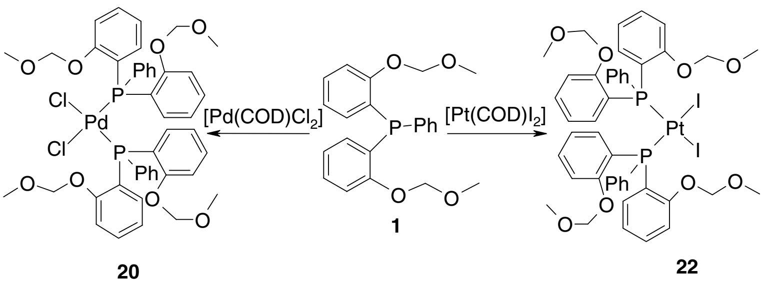

Scheme 3.

Table 7
^{1}H and ^{31}P NMR data of compounds **1**–**21**

Compounds	δ_{CH_3}	δ_{CH_2}	δ_P	J_{PM}	$\Delta\delta$
PPh$_2$C$_6$H$_4$OCH$_2$CH$_3$ (**1**)	–	–	−16.0	–	–
PPh(C$_6$H$_4$OCH$_2$CH$_3$)$_2$ (**2**)	–	–	−26.1	–	–
[Cr(CO)$_4$(PPh$_2$C$_6$H$_4$OCH$_2$CH$_3$)$_2$] (**3**)	3.05	4.89	70.7	–	86.7
[Cr(CO)$_4${PPh(C$_6$H$_4$OCH$_2$CH$_3$)$_2$}$_2$] (**4**)	3.19	5.11	68.3	–	94.4
[Mo(CO)$_4$(PPh$_2$C$_6$H$_4$OCH$_2$CH$_3$)$_2$] (**5**)	3.10	4.99	33.7	–	49.7
[W(CO)$_4$(PPh$_2$C$_6$H$_4$OCH$_2$CH$_3$)$_2$] (**6**)	3.23	5.14	18.2	229	34.2
[W(CO)$_4${PPh(C$_6$H$_4$OCH$_2$CH$_3$)$_2$}$_2$] (**7**)	3.09	4.85	17.8	259	43.9
[Mo(CO)$_5$(PPh$_2$C$_6$H$_4$OCH$_2$CH$_3$)] (**8**)	3.09	4.99	29.5	–	45.5
[Mo(CO)$_5${PPh(C$_6$H$_4$OCH$_2$CH$_3$)$_2$}] (**9**)	3.12	5.02	22.6	–	48.7
[Ru(Ph$_2$PC$_6$H$_4$O)$_3$] (**10**)	–	–	49.1	–	76.2
[Rh(CO)Cl(PPh$_2$C$_6$H$_4$OCH$_2$OCH$_3$)] (**12**)	1.25	2.17	59.5	174	75.5
[Rh(COD)(PPh$_2$C$_6$H$_4$OCH$_2$OCH$_3$)Cl] (**13**),	3.37	5.07	23.0	150	39.0
[Rh(COD)(PPh$_2$C$_6$H$_4$OCH$_2$OCH$_3$)]$_2$ · 2Cl (**14**)	1.38	2.59	48.4	142	64.4
[Rh(COD)(PPh$_2$C$_6$H$_4$OCH$_2$OCH$_3$)]$^{\cdot}$BF$_4$ (**15**)	1.43	2.19	34.0	159	50.0
[Pd(PPh$_2$C$_6$H$_4$O)(PPh$_2$C$_6$H$_4$OH)Cl] (**16**)	–	–	20.8(d), 47.1(d)	12.3[a]	47.9, 74.2
[Pd(PPh$_2$C$_6$H$_4$O)$_2$] (**17**)	–	–	43.7	–	70.8
[Pd(PPh$_2$C$_6$H$_4$OCH$_2$OCH$_3$)$_2$] · 2BF$_4$ (**19**)	0.90	2.20	45.4	–	61.4
[Pd{Ph(C$_6$H$_4$OCH$_2$OCH$_3$)$_2$}$_2$Cl$_2$] (**20**)	3.05	4.85	14.3	–	40.4
[Pt(PPh$_2$C$_6$H$_4$OCH$_2$OCH$_3$)$_2$I$_2$] (**21**)	3.10	4.94	5.6	2565	21.6
[Pt{PPh(C$_6$H$_4$OCH$_2$OCH$_3$)$_2$}$_2$I$_2$] (**22**)	3.11	4.94	1.7	2611	27.8

[a] $^2J_{PP}$; δ in ppm and J in Hz.

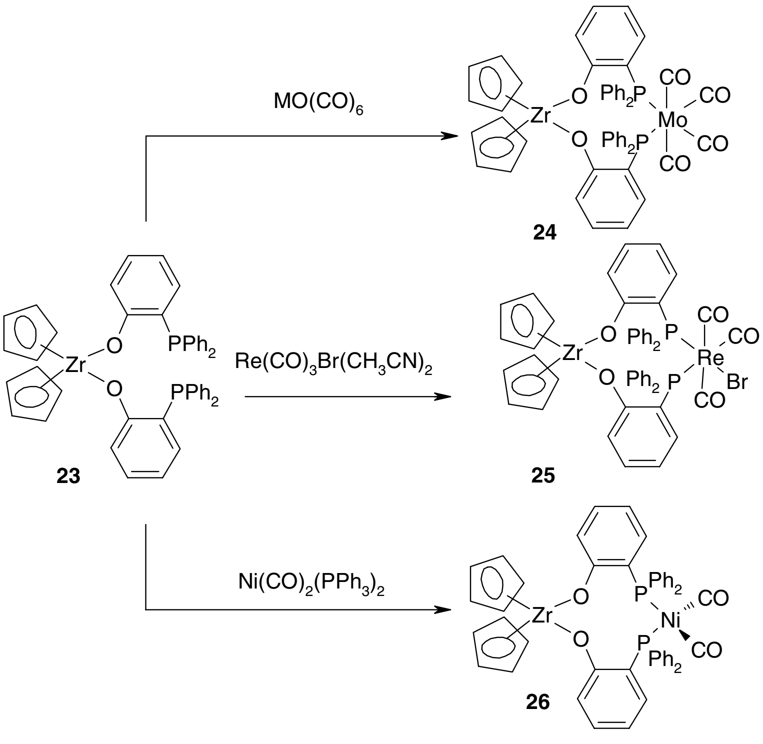

Scheme 4.

linkage gets cleaved in case of Ru(III), Ru(II) and Pd(II) derivatives. This could be attributed to the presence of additional ‘OCH$_2$’ group, which facilitates the metathetical elimination of methoxymethyl chloride. The crystal structure of the palladium complex shows extensive hydrogen bonding between the co-crystallized phosphonium salt and the metal moiety. Besides the cleavage, the quaternization of phosphorus center was also observed in the formation of the phosphonium salt (**18**) which was found co-crystallized with palladium complex **16**.

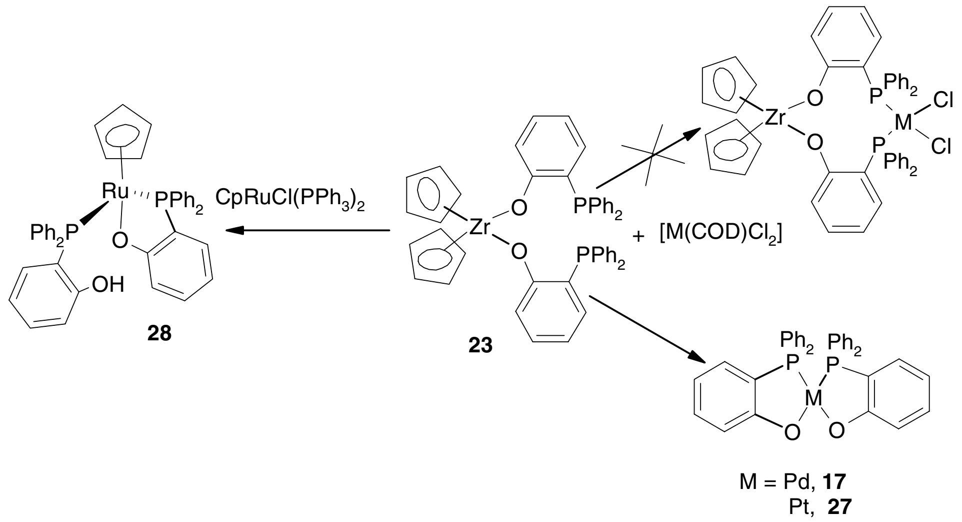

Scheme 5.

Interestingly, the formation of phosphonium salt, presumably from the cleavage product, CH_3OCH_2Cl, appears to take place only in the presence of a metal. No such reaction was observed in the deprotection reactions of ligands **1** or **2** with anhydrous HCl where the byproduct is also CH_3OCH_2Cl. The extensive hydrogen-bonding interactions between the phosphonium salt and the hydroxyl group on the palladium bound phosphinophenol of complex **17** prevented the formation of complex **18** through cyclization.

The metalloligand $Cp_2Zr(OC_6H_4PPh_2)_2$ obtained from phosphinophenol readily forms heterobimetallic complexes, $[(OC)_4Mo(\mu\text{-}PPh_2C_6H_4O\text{-}o)_2ZrCp_2]$, *mer*-$[(OC)_3Re(\mu\text{-}PPh_2C_6H_4O\text{-}o)_2ZrCp_2]$ and $[(OC)_2Ni(\mu\text{-}PPh_2C_6H_4O\text{-}o)_2ZrCp_2]$ with corresponding metal carbonyl derivatives. Its reactions with the metal halides leads to *trans* metallation and formation of chelate complexes $[M(Ph_2PC_6H_4O\text{-}o)_2]$ (M = Pd, Pt) and $[CpRu(PPh_2C_6H_4OH\text{-}o)(PPh_2C_6H_4O\text{-}o)]$. The Group 6 metal derivatives with free ether ends can be used as metallo ligands to prepare homo- and heterobimetallic complexes. The Rh(I) and heterobimetallic complexes reported here give scope for utilization as catalysts in various organic transformations. The research in this direction is in progress in our laboratory.

4. Experimental

All manipulations were performed under rigorously anaerobic conditions using Schlenk techniques. All the solvents were purified by conventional procedures and distilled prior to use. The phosphine ethers $Ph_2PC_6H_4OCH_2OCH_3\text{-}o$ [7] and $PhP(C_6H_4OCH_2OCH_3\text{-}o)_2$ [7] and metal precursors, $M(CO)_4(NBD)$ (M = Mo [13], Cr [14]) and $W(CO)_4(pip)_2$ [15] $M(COD)Cl_2$ (M = Pd [16], Pt [17]), $[Rh(CO)_2Cl]_2$ [18] and $[Rh(COD)Cl]_2$ [19] were prepared according to the literature procedures. The ^1H and ^{31}P NMR spectra were recorded using VXR 300 S and Bruker spectrometers; Me_4Si was used as internal standard for the ^1H NMR and 85% H_3PO_4 as external standard for the ^{31}P NMR. Positive values indicate downfield shifts. IR spectra were recorded on a Nicolet Impact 400 FT IR instrument in KBr disks. Microanalyses were performed on a Carlo Erba model 1112 elemental analyser. The FAB mass spectra were recorded on JEOL SX 102/DA-6000 and Q-Tof micro (YA-105) mass spectrometer/Data system using Argon/Xenon (6 kV, 10 mA) as FAB gas. Melting points were recorded in capillary tubes and are uncorrected.

4.1. *trans*-$[Cr(CO)_4(RPPhC_6H_4OCH_2OCH_3\text{-}o)_2]$ (R = Ph, *3*; $C_6H_4OCH_2OCH_3$-*o*, *4*)

A mixture of $Cr(CO)_4(NBD)$ (0.035 g, 0.136 mmol) and $RPPhC_6H_4OCH_2OCH_3\text{-}o$ (0.270 mmol) in *n*-hexane (10 ml) was heated to reflux for 9 h. The reaction mixture became turbid and the yellow solid precipitated out was filtered and the precipitate was dried and recrystallized from CH_2Cl_2–diethyl ether (2:1) mixture to obtain pure products.

4.2. *trans*-$[Cr(CO)_4(PPh_2C_6H_4OCH_2OCH_3\text{-}o)_2]$ (*3*)

Yield: 59% (0.097 g, 0.113 mmol), m.p.: 152–156 °C (dec.). Anal. Calc. for $C_{44}H_{38}O_8P_2Cr$: C 65.35; H 4.74. Found: C 65.14; H 4.62%. FTIR (KBr disk) cm^{-1}: ν_{CO}: 1887 vs. ^1H NMR ($CDCl_3$): δ 3.05 (s, CH_3, 3H), 4.89 (s, CH_2, 2H), 6.64–7.65 (m, *phenyl*, 14H). $^{31}P\{^1H\}$ NMR ($CDCl_3$): δ 70.7 (s).

4.3. *trans-[Cr(CO)$_4${PPh(C$_6$H$_4$OCH$_2$OCH$_3$-o)$_2$}$_2$] (**4**)*

Yield: 63% (0.091 g, 0.098 mmol), m.p.: 128–130 °C (dec.). Anal. Calc. for $C_{48}H_{46}O_{12}P_2Cr$: C 62.07; H 4.99. Found: C 61.92; H 5.17%. FTIR (KBr disk) cm^{-1}: ν_{CO}: 1877 vs. ^{1}H NMR (CDCl$_3$): 3.19 (s, C*H*$_3$, 6H), 5.11 (s, C*H*$_2$, 4H), 6.64–7.65 (m, *phenyl*, 13H). ^{31}P{^{1}H} NMR (CDCl$_3$): δ 68.3 (s).

4.4. *Mo(CO)$_4$(PPh$_2$C$_6$H$_4$OCH$_2$OCH$_3$-o)$_2$ (**5**)*

A solution of Mo(CO)$_4$(NBD) (0.04 g, 0.130 mmol) in *n*-hexane (5 ml) was added to $Ph_2PC_6H_4OCH_2OCH_3$-*o* (0.088 g, 0.260 mmol) in *n*-hexane (5 ml) and was heated to reflux for 2 h. The yellow solid precipitated out from the reaction mixture was separated by filtration and the residue was washed with *n*-hexane and dried under vacuum. Yield: 85% (0.097 g, 0.113 mmol), m.p.: 154–156 °C (dec.). Anal. Calc. for $C_{44}H_{38}O_8P_2Mo \cdot CH_2Cl_2$: C 57.65; H 4.30. Found: C 57.28; H 4.40%. FTIR (KBr disk) cm^{-1}: ν_{CO}: 2014 s, 1916 vs, 1883 vs. ^{1}H NMR (CDCl$_3$): δ 3.10 (s, C*H*$_3$, 3H), 4.99 (s, C*H*$_2$, 2H), 6.69–7.73 (m, *phenyl*, 14H). ^{31}P{^{1}H} NMR (CDCl$_3$): δ 33.7 (s).

4.5. *cis-[W(CO)$_4$(RPPhC$_6$H$_4$OCH$_2$OCH$_3$-o)$_2$] (R = Ph, **6**; C$_6$H$_4$OCH$_2$OCH$_3$-o, **7**)*

To a solution of $RPhPC_6H_4OCH_2OCH_3$-*o* (0.214 mmol) in CH$_2$Cl$_2$ (5 ml) was added a solution of W(CO)$_4$(NC$_5$H$_{11}$)$_2$ (0.050 g, 0.102 mmol) also in CH$_2$Cl$_2$ (5 ml) at room temperature and the reaction mixture was stirred at room temperature for 12 h. The solvent was evaporated from the reaction mixture under reduced pressure and the residue obtained was washed with *n*-hexane (5 × 5 ml) and re-crystallized from a mixture of CH$_2$Cl$_2$-*n*-hexane (1:1) to obtain analytically pure product.

4.6. *cis-[W(CO)$_4$(PPh$_2$C$_6$H$_4$OCH$_2$OCH$_3$-o)$_2$] (**6**)*

Yield: 85% (0.085 g, 0.090 mmol), m.p.: 154–157 °C (dec.). Anal. Calc. for $C_{44}H_{38}O_8P_2W$: C 56.19; H 4.07. Found: C 56.29; H 3.98%. FTIR (KBr disk) cm^{-1}: ν_{CO}: 2010 s, 1927 vs, 1876 vs, 1774s. ^{1}H NMR (CD$_3$COCD$_3$): 3.23 (s, C*H*$_3$, 3H), 5.14 (s, C*H*$_2$, 2H), 7.08–7.82 (m, *phenyl*, 14H). ^{31}P{^{1}H} NMR (CD$_3$COCD$_3$): δ 18.2 ($^1J_{WP}$ = 229.2 Hz).

4.7. *cis-[W(CO)$_4${PPh (C$_6$H$_4$OCH$_2$OCH$_3$-o)$_2$}$_2$] (**7**)*

Yield: 84% (0.095 g, 0.080 mmol), m.p.: 117–120 °C (dec.). Anal. Calc. for $C_{48}H_{46}O_{12}P_2W$: C 54.33; H 4.37. Found: C 53.92; H 4.47%. FTIR (KBr disk) cm^{-1}: ν_{CO}: 2009 s, 1912 vs, 1876 vs, 1850s. ^{1}H NMR (CDCl$_3$): δ 3.09 (s, C*H*$_3$, 6H), 4.85 (s, C*H*$_2$, 4H), 6.82–7.42 (m, *phenyl*, 13H). ^{31}P{^{1}H} NMR (CDCl$_3$): δ 17.8 ($^1J_{WP}$ = 259.2 Hz).

4.8. *Mo(CO)$_5$(RPPhC$_6$H$_4$OCH$_2$OCH$_3$-o) (R = Ph, **8**; C$_6$H$_4$OCH$_2$OCH$_3$-o, **9**)*

A mixture of Mo(CO)$_6$ (0.05 g, 0.176 mmol) and $PhPC_6H_4OCH_2OCH_3$-*o* (0.176 mmol) in benzene (10 ml) was refluxed for 20 h. The solvent was evaporated under reduced pressure and the residue obtained was extracted with *n*-hexane (3 × 5 ml). The solution was filtered through celite, the yellow filtrate was concentrated to 4 ml and cooled at 0 °C to give crystalline products.

4.9. *Mo(CO)$_5$(PPh$_2$C$_6$H$_4$OCH$_2$OCH$_3$-o) (**8**)*

Yield: 48% (0.052 g, 0.093 mmol), m.p.: 134–136 °C (dec.). Anal. Calc. for $C_{25}H_{19}O_7PMo$: C 53.79; H 3.43. Found: C 53.68; H 3.55%. FTIR (KBr disk) cm^{-1}: ν_{CO}: 2071 s, 1931 br and vs. ^{1}H NMR (CDCl$_3$): δ 3.09 (s, OC*H*$_3$, 3H), 4.99 (s, OC*H*$_2$, 2H), 6.87–7.62 (m, *phenyl*, 14H). ^{31}P{^{1}H} NMR (CDCl$_3$): δ 29.5 (s).

4.10. *Mo(CO)$_5${PPh(C$_6$H$_4$OCH$_2$OCH$_3$-o)$_2$} (**9**)*

Yield: 81% (0.095 g, 0.154 mmol), m.p.: 114–116 °C (dec.). Anal. Calc. for $C_{27}H_{23}O_9PMo$: C 52.45; H 3.75. Found: C 52.26; H 3.68%. FTIR (KBr disk) cm^{-1}: ν_{CO}: 2066 s, 1943 br and vs. ^{1}H NMR (CDCl$_3$): δ 3.12 (s, OC*H*$_3$, 6H), 5.02 (AB q, OC*H*$_2$, $^2J_{HH}$ = 7.12 Hz, 4H), 6.95–7.62 (m, *phenyl*, 13H). ^{31}P{^{1}H} NMR (CDCl$_3$): δ 22.6 (s).

4.11. *[Ru(OC$_6$H$_4$PPh$_2$)$_3$] (**10**)*

To a refluxing solution of $Ph_2PC_6H_4OCH_2OCH_3$ (0.186 g, 0.570 mmol) in 2-methoxyethanol (5 ml) was added $RuCl_3 \cdot 3H_2O$ (0.05 g, 0.190 mmol) in water (2 ml) and the reaction mixture was refluxed for 2 h. The reaction mixture was filtered to separate a blue crystalline solid and further product was obtained from the mother liquor on concentration and cooling. Single crystals of the product were grown by slow evaporation of a CH$_2$Cl$_2$ solution at room temperature. Yield: 70% (0,135 g, 0.130 mmol), m.p.: above 250 °C (dec.). Anal. Calc. for $C_{54}H_{42}P_3O_3Ru \cdot CH_2Cl_2$: C 64.90; H 4.36. Found: C 64.68; H 4.26%. ^{1}H NMR (CDCl$_3$): 6.0–8.7 (m, *phenyl*) (broad). ^{31}P{^{1}H} NMR (CDCl$_3$): broad peak centered at 49 ppm.

4.12. *CpRu(OC$_6$H$_4$PPh$_2$)(PPh$_3$)$_2$ (**11**)*

To a solution of CpRuCl(PPh$_3$)$_2$ (0.05 g, 0.068 mmol) in CH$_2$Cl$_2$ (5 ml) was added a CH$_2$Cl$_2$ (5 ml) solution of **1** (0.022 g, 0.068 mmol) and the reaction mixture was stirred at room temperature for 6 h. The resulting solution was evaporated under reduced pressure and the residue was with *n*-hexane (3 × 5 ml), the residue was dissolved in toluene (10 ml) and the solution on storing at 0 °C gave orange-red crystalline product. Yield: 40% (0.021 g, 0.029 mmol), m.p.: 168–170 °C (dec.). Anal. Calc. for $C_{41}H_{34}OP_2Ru$: C 69.78; H 4.86. Found: C 69.03; H 4.67%. ^{1}H NMR ($CDCl_3$): δ 4.10 (s, C_5H_5, 5H), 6.85–7.04 (m, *phenyl*, 4H), 7.11–7.72 (m, P*Ph*, 25H). $^{31}P\{^1H\}$ NMR ($CDCl_3$): δ 44.2 (d, *P*Ph_3, $^2J_{PRuP}$ = 36.4 Hz), 57.4 (d, *P*Ph_2, $^2J_{PRuP}$ = 36.4 Hz). MS (FAB): 706 (M^+ + 1).

4.13. *[Rh(CO)(PPh$_2$C$_6$H$_4$OCH$_2$OCH$_3$)Cl]* (**12**)

A mixture of $[Rh(CO)_2Cl]_2$ (0.030 g, 0.077 mmol) and $Ph_2PC_6H_4OCH_2OCH_3$ (0.05 g, 0.154 mmol) in CH_3CN (10 ml) was stirred at reflux for 4 h. The resulting yellow solution was evaporated under reduced pressure and the residue was crystallized from a CH_2Cl_2-*n*-hexane (2:1) mixture at −10 °C to get the product of analytical purity. Yield: 76% (0.057g, 0.117 mmol), m.p.: 195–198 °C (dec.). Anal. Calc. for $C_{21}H_{19}O_3PRhCl$, C 51.61; H 3.92. Found: C 51.47; H 3.87%. FTIR (KBr disk) cm^{-1}: ν_{CO}: 1956 vs. ^{1}H NMR ($CDCl_3$): δ 1.25 (s, OC*H*$_3$, 3H), 2.17 (s, OC*H*$_2$, 2H), 7.26–7.76 (m, *phenyl*, 14H). $^{31}P\{^1H\}$ NMR ($CDCl_3$): δ 59.5 (d, $^1J_{RhP}$ = 173.8 Hz).

4.14. *[RhCl(COD)(PPh$_2$C$_6$H$_4$OCH$_2$OCH$_3$)]* (**13**)

A mixture of $[Rh(COD)Cl]_2$ (0.025 g, 0.051 mmol) and $PPh_2C_6H_4OCH_2CH_3$ (0.033 g, 0.104 mmol) in CH_3CN (10 ml) was stirred with heating for 10 h. The reaction mixture was cooled, the solvent was evaporated under reduced pressure and the residue obtained was washed with *n*-hexane (5 × 3 ml) and dried to get yellow solid of analytical purity. Yield: 67% (0.050 g, 0.068 mmol), m.p.: 149–155 °C (dec.). Anal. Calc. for $C_{28}H_{31}O_2PRhCl \cdot 2CH_2Cl_2$: C 48.77; H 4.78. Found: C 48.34; H 4.57%. ^{1}H NMR ($CDCl_3$): δ 1.64–2.47 (m, C*H*$_2$ (COD), 8H), 3.37 (br s, OC*H*$_3$ and =CH (COD), 4H), 4.23 (br, =C*H* (COD), 1H), 5.07 (s, OC*H*$_2$, 2H), 5.43 (s, =C*H* (COD), 2H), 6.93–7.82 (m, *phenyl*, 14H). $^{31}P\{^1H\}$ NMR ($CDCl_3$): δ 23.0 (d, $^1J_{RhP}$ = 149.6 Hz).

The ^{31}P NMR spectrum of the crude sample showed two peaks [$^{31}P\{^1H\}$ NMR ($CDCl_3$): δ 23.0 (d, $^1J_{RhP}$ = 149.6 Hz), 48.4 (d, $^1J_{RhP}$ = 141.9 Hz)]. The additional doublet at 48.4 ppm could be eliminated by crystallization and the presence of that may be attributed to the complex $[Rh(COD)(PPh_2C_6H_4OCH_2CH_3–\kappa P, \kappa O)]_2Cl_2$ (**14**).

4.15. *[Rh(COD)(PPh$_2$C$_6$H$_4$OCH$_2$OCH$_3$)]BF$_4$* (**15**)

To a mixture of $[Rh(COD)Cl]_2$ (0.025 g, 0.051 mmol) and $PPh_2C_6H_4OCH_2CH_3$ (0.033 g, 0.104 mmol) in acetone (10 ml), $AgBF_4$ (0.0197 g, 0.100 mmol) was added and the reaction mixture was stirred at room temperature for 6 h and passed through celite. The filtrate was evaporated under reduced pressure and the residue was washed with petroleum ether (3 × 5 ml) and crystallized from a CH_2Cl_2/petroleum ether mixture (2:1) at 0 °C to give crystalline product. Yield: 72% (0.045 g, 0.07 mmol), m.p.: 166–170 °C (dec.). Anal. Calc. for $C_{28}H_{31}O_2PRhBF_4$: C 54.22; H 5.04. Found: C 53.99; H 4.95%. ^{1}H NMR ($CDCl_3$): δ 0.83–1.31 (m, C*H*$_2$ (COD), 8H), 1.43 (s, OC*H*$_3$, 3H), 2.19 (s, OC*H*$_2$, 2H), 2.47 (br, =C*H* (COD), 2H), 3.81 (br, =CH (COD), 1H), 5.71 (br, =C*H* (COD), 1H), 6.83–7.74 (m, *phenyl*, 14H). $^{31}P\{^1H\}$ NMR ($CDCl_3$): δ 34.0 (d, $^1J_{RhP}$ = 159.2 Hz).

4.16. *Reaction of [Pd(COD)Cl$_2$] with* **1**

To a stirred solution of $Ph_2PC_6H_4OCH_2OCH_3$ (0.068 g, 0.210 mmol) in CH_2Cl_2 (5 ml) was added drop-wise a solution of *cis*-$Pd(COD)Cl_2$ (0.030 g, 0.210 mmol) also in CH_2Cl_2 (5 ml) at room temperature and the reaction mixture was stirred at room temperature for 8 h. Solvent was evaporated under reduced pressure from the reaction mixture and the residue obtained was washed with *n*-hexane (3 × 5 ml). The phosphorus NMR of the crude solid revealed the presence of mixture of products [$^{31}P\{^1H\}$ NMR ($CDCl_3$): δ 20.8 (d), 47.1(d) (*P*Ph_2, $^2J_{PP}$ = 12.3 Hz); 16.1 (s); 43.7 (s)]. Recrystallization of this mixture at room temperature from CH_2Cl_2/diethyl ether (2:1) mixture at room temperature, afforded yellow crystalline $[Pd(PPh_2C_6H_4O)_2]$ (**17**) in the first crop and from the mother liquor on cooling yellow crystals of the complex **16** co-crystallized with $Ph_2P^+(CH_2OCH_3)(C_6H_4OH)Cl$ (**18**).

4.17. *[PdCl(PPh$_2$C$_6$H$_4$OH)(PPh$_2$C$_6$H$_4$O)]* (**16**)

Yield: 40% (0.044 g, 0.042 mmol), m.p.: 155–158 °C. Anal. Calc. for $C_{36}H_{29}O_2P_2PdCl_2$. $C_{20}H_{20}O_2PCl$, C 63.68; H 4.67. Found: C 63.38; H 4.61%. ^{1}H NMR ($CDCl_3$): δ 1.95 (s, C*H*$_3$, 3H), 3.51 (br s, OC*H*$_2$, 2H), 6.45–7.98 (m, *phenyl*, 28H). $^{31}P\{^1H\}$ NMR ($CDCl_3$): δ 20.8 (d), 47.1(d) (*P* Ph_2, $^2J_{PP}$ = 12.3 Hz); 16.0 (s). $[Pd(\eta^2\text{-}PPh_2C_6H_4O)_2]$ (**17**). Yield: 21% (0.015 g, 0.022 mmol), m.p.: 225–227 °C. Anal. Calc. for $C_{37.5}H_{31}Cl_3O_2P_2Pd$: C 57.13; H 3.96. Found: C 57.25; H 4.01%. $^{31}P\{^1H\}$ NMR ($CDCl_3$): δ 43.7 (s). MS (FAB): 661 (M^+ + 1).

4.18. *[Pd(PPh$_2$C$_6$H$_4$OCH$_2$OCH$_3$)$_2$](BF$_4$)$_2$* (**19**)

To a stirring solution of $Ph_2PC_6H_4OCH_2O–CH_3$ (0.068 g, 0.210 mmol) and $AgBF_4$ (0.041 g, 0.210 mmol) in CH_2Cl_2 (5 ml) was added *cis*-$Pd(COD)Cl_2$ (0.030 g, 0.210 mmol) also in CH_2Cl_2 (5 ml) at room temperature. The reaction mixture was stirred at room temperature for 6 h. The resulting solution was passed through celite, the solvent was evaporated in vacuo and the residue obtained was washed with *n*-hexane (3 × 5 ml). The yellow solid was crystallized from a CH_2Cl_2/*n*-hexane (2:1) mixture at 0 °C to give bright yellow crystalline solid **19**.

Yield: 65% (0.063 g, 0.068 mmol), m.p.: 208–211 °C. Anal. Calc. for $C_{40}H_{38}O_4P_2PdB_2F_8$: C 51.96; H 4.14. Found: C 51.83; H 4.22%. ^1H NMR ($CDCl_3$): δ 0.90 (s, OC*H*$_3$, 3H), 2.20 (s, OC*H*$_2$, 2H), 6.78–7.82 (m, *phenyl*, 14H). $^{31}P\{^1H\}$ NMR ($CDCl_3$): δ 45.4 (s). MS (FAB): 927 (M^+ + 2).

4.19. *[$PdCl_2\{PPh(C_6H_4OCH_2OCH_3)_2\}_2$]* (**20**)

To a stirring solution of $PhP(C_6H_4OCH_2OCH_3)_2$ (0.080 g, 0.210 mmol) in CH_2Cl_2 (5 ml) was added a solution of *cis*-Pd(COD)Cl_2 (0.030 g, 0.210 mmol) also in CH_2Cl_2 (5 ml) at room temperature and the resulting yellow solution was stirred at room temperature for 6 h. Solvent was evaporated under reduced pressure from the reaction mixture, the residue was washed with *n*–hexane (3 × 5 ml) and was crystallized from CH_2Cl_2/*n*-hexane (2:1) mixture at 0 °C to give a bright yellow crystalline solid. Yield: 61% (0.067 g, 0.064 mmol), m.p.: 220–222 °C. Anal. Calc. for $C_{44}H_{46}O_4P_2PdCl_2 \cdot 2CH_2Cl_2$: C 52.72; H 4.80. Found: C 52.79; H 4.66%. ^1H NMR ($CDCl_3$): δ 3.05 (s, OC*H*$_3$, 3H), 4.85 (s, OC*H*$_2$, 2H), 6.93–7.83 (m, *phenyl*, 13H). $^{31}P\{^1H\}$ NMR ($CDCl_3$): δ 14.3 (s).

4.20. *[$PtI_2(P(R)PhC_6H_4OCH_2OCH_3)_2$] (R = Ph, 21; $C_6H_4OCH_2CH_3$, 22)*

To a stirring solution of *cis*-Pt(COD)I_2 (0.030 g, 0.054 mmol) in CH_2Cl_2 (5 ml), $PhRPC_6H_4OCH_2OCH_3$ (0.108 mmol) in CH_2Cl_2 (5 ml) was added at room temperature and the reaction mixture was stirred at room temperature for 6 h. The solvent was evaporated from the reaction mixture under reduced pressure and the residue obtained was washed with *n*-hexane (3 × 5 ml) and re-crystallized from CH_2Cl_2/*n*-hexane (2:1) mixture at 0 °C to give a bright yellow crystalline product.

4.21. *[$PtI_2(PPh_2C_6H_4OCH_2OCH_3)_2$]* (**21**)

Yield: 59% (0.040g, 0.032 mmol), m.p.: 228–230 °C (dec.). Anal. Calc. for $C_{40}H_{38}O_4P_2PtI_2 \cdot 2CH_2Cl_2$: C39.93; H 3.35. Found: C 39.58; H 2.85%. ^1H NMR ($CDCl_3$): δ 3.10 (s, OC*H*$_3$, 3H), 4.94 (s, OC*H*$_2$, 2H), 6.92–7.87 (m, *phenyl*, 14H). $^{31}P\{^1H\}$ NMR ($CDCl_3$): δ 5.6 ($^1J_{PtP}$ = 2565 Hz).

4.22. *[$PtI_2\{PPh(C_6H_4OCH_2OCH_3)_2\}_2$]* (**22**)

Yield: 68% (0.048g, 0.036 mmol), m.p.: 198–201 °C (dec.). Anal. Calc. for $C_{40}H_{46}O_8P_2PtI_2$: C 41.21; H 3.97. Found: C 41.04; H 3.99%. ^1H NMR ($CDCl_3$): δ 3.11 (s, OC*H*$_3$, 3H), 4.94 (s, OC*H*$_2$, 2H), 6.89–7.86 (m, *phenyl*, 13H). $^{31}P\{^1H\}$ NMR ($CDCl_3$): δ 1.7 ($^1J_{PtP}$ = 2611 Hz).

4.23. *$(OC)_4Mo(\mu\text{-}PPh_2C_6H_4O)_2ZrCp_2$* (**24**)

To a solution of $Cp_2Zr(OC_6H_4PPh_2)_2$ (0.088 g, 0.11 mmol) in benzene (5 ml) was added $Mo(CO)_6$ (0.03 g, 0.11 mmol) also in benzene (5 ml) and the reaction mixture was stirred at reflux condition for 10 h. The solvent was evaporated under reduced pressure and the residue obtained was extracted with petroleum ether (15 ml) and the solution was passed through celite. The filtrate on concentration and cooling gave yellow crystalline product. Yield: 45% (0.05 g, 0.051 mmol), m.p.: 160–164 °C (dec.). Anal. Calc. for $C_{50}H_{38}O_6P_2MoZr$: C 61.03; H 3.89. Found: C 61.18; H 3.96%. FTIR (KBr disk) cm^{-1}: ν_{CO}: 2014 m, 1922 s, 1875 s, 1842 s. ^1H NMR ($CDCl_3$): 5.81 (s, C_5*H*$_5$, 5H), 6.79–7.19 (m, *phenyl*, 4H), 7.26–7.92 (m, P*Ph*$_2$, 10H). $^{31}P\{^1H\}$ NMR ($CDCl_3$): 39.5(s). MS (FAB): 988 (M^+).

4.24. *mer-$(OC)_3ReBr(\mu\text{-}PPh_2C_6H_4O)_2ZrCp_2$* (**25**)

To a stirring solution of $Cp_2Zr(OC_6H_4PPh_2)_2$ (0.072 g, 0.09 mmol) in CH_2Cl_2 (7 ml) was added drop wise a solution of *fac*-[$Re(CO)_3(CH_3CN)_2Br$] (0.04 g, 0.09 mmol) also in CH_2Cl_2 (5 ml) at room temperature and the reaction mixture was allowed to stir at room temperature for 3 h. The solution was concentrated, diluted with *n*-hexane (3 ml) and cooled to 0 °C to give crystalline product of **24**. Yield: 83% (0.087 g, 0.076 mmol). Anal. Calc. for $C_{49}H_{38}BrO_5P_2ReZr$: C 52.26; H 3.40. Found: C 52.12; H 3.31%. FTIR (KBr disk) cm^{-1}: ν_{CO}: 2029 vs, 1949 s, 1899 vs. ^1H NMR ($CDCl_3$): δ 6.37 (s, C_5*H*$_5$, 5H), 6.48–6.82 (m, *phenyl*, 4H), 7.03–7.61 (m, P*Ph*$_2$, 14H). $^{31}P\{^1H\}$ NMR ($CDCl_3$): δ 9.5 (d), 26.5 (d); ($^2J_{PReP}$ = 29.7 Hz.). MS (FAB): 1123.9 (M^+).

4.25. *$(OC)_2Ni(\mu\text{-}PPh_2C_6H_4O)_2ZrCp_2$* (**26**)

To a solution of $Cp_2Zr(OC_6H_4PPh_2)_2$ (0.048 g, 0.06 mmol) in CH_2Cl_2 (5 ml) was added drop wise a solution of $Ni(CO)_2(PPh_3)_2$ (0.04 g, 0.60 mmol) also in CH_2Cl_2 (5 ml) and the reaction mixture was stirred at room temperature for 6 h. The solvent was removed under reduced pressure and the residue obtained was washed with *n*-hexane (3 × 5 ml) and re-crystallized from CH_2Cl_2–petroleum ether (2:1) mixture at −5 °C to get crystalline product of **25**. Yield: 91% (0.05 g, 0.056 mmol), m.p.: 225–228 °C (dec.). Anal. Calc. for $C_{48}H_{38}BrO_4P_2NiZr$: C 59.40; H 3.95. Found: C 59.22; H 3.82%. FTIR (KBr disk) cm^{-1}: ν_{CO}: 2004 s, 1948 s. ^1H NMR ($CDCl_3$): 6.72 (s, C_5*H*$_5$, 5H), 6.93–7.69 (m, *phenyl*, 14H). $^{31}P\{^1H\}$ NMR ($CDCl_3$): 34.4 (s). MS (FAB): 890 (M^+).

4.26. *Pd\{$(OC_6H_4PPh_2)_2$\}* (**17**)

A mixture of *cis*-[$PdCl_2(COD)$] (0.03 g, 0.105 mmol) and $Cp_2Zr(OC_6H_4PPh_2)_2$ (0.082 g, 0.11 mmol) was dissolved in 7 ml of dichloromethane and the solution was stirred at room temperature for 6 h. Evaporation of the solution under vacuo yielded sticky residue, which was washed with petroleum ether twice to remove cyclooctadiene. The resultant crude bright-yellow solid obtained was crystallized from a CH_2Cl_2–petroleum ether (3:1) mixture. Yield: 70% (0.07 g, 0.073 mmol), m.p.: 225–227 °C (dec.). ^1H NMR ($CDCl_3$): δ 6.57–6.91 (m, phenyl, 4H), 7.03–8.71 (m, *phenyl*, 10H). $^{31}P\{^1H\}$ NMR ($CDCl_3$): δ 43.7 (s).

4.27. $Pt\{(OC_6H_4PPh_2)_2\}$ (**27**)

A mixture of *cis*-[$PtCl_2(COD)$] (0.03 g, 0.08 mmol) and $Cp_2Zr(OC_6H_4PPh_2)_2$ (0.062 g, 0.08 mmol) was dissolved in 5 ml of dichloromethane and the solution was stirred for 6 h at room temperature. Evaporation of the reaction mixture under vacuo yielded sticky white residue, which was washed with diethyl ether (2 × 4 ml). The resultant crude bright-white solid was dissolved in a mixture of CH_2Cl_2–petroleum ether (3:1) mixture to give analytically pure sample of **27**. Yield: 70% (0.058 g, 0.053 mmol). Anal. Calc. for $C_{36}H_{28}O_2P_2Pt$: C 62.87; H 4.10. Found: C 62.82; H 4.12%. ^1H NMR ($CDCl_3$): δ 6.49 (t, O–C_6H_4–P, $^3J_{HH}$ = 8.9 Hz, 2H), 6.88 (t, O–C_6H_4–P, $^3J_{HH}$ = 8.9 Hz, 2H), 7.02–7.36 (m, P*Ph*, 10H). $^{31}P\{^1H\}$ NMR ($CDCl_3$): δ 19.3 (s, $^1J_{PtP}$ = 3540 Hz).

4.28. $CpRu(PPh_2C_6H_4O)(PPh_2C_6H_4OH)$ (**28**)

To a solution of **23** (0.053 g, 0.068 mmol) in CH_2Cl_2 (5 ml) was added a solution of $CpRuCl(PPh_3)_2$ (0.05 g, 0.068 mmol) also in CH_2Cl_2 (5 ml) and the reaction mixture was stirred at room temperature for 12 h. The solution was evaporated under reduced pressure and the residue obtained was dissolved in diethyl ether (10 ml), which on cooling gave orange-red crystalline product of **27**. Yield: 61% (0.031 g, 0.043 mmol), m.p.: 177–180 °C (dec.). Anal. Calc. for $C_{41}H_{34}O_2P_2Ru$: C 68.23; H 4.75. Found: C 69.01; H 5.18%. FTIR (KBr disk) cm^{-1}: ν_{OH}: 3404 br s. ^1H NMR ($CDCl_3$): δ 4.22 (s, C_5H_5, 5H), 6.29–6.92 (m, *phenyl*, 8H), 7.02–7.45 (m, P*Ph*, 20H). $^{31}P\{^1H\}$ NMR ($CDCl_3$): δ 45.2 (d, *P*Ph_2, $^2J_{PRuP}$ = 37.8 Hz), 63.9 (d, *P*Ph_2, $^2J_{PRuP}$ = 37.8 Hz). MS (FAB): 722 (M^+ + 1), 705 (M^+–OH).

4.29. $CpRu(PPh_2C_6H_4O)(PPh_3)_2$ (**11**)

To a solution of $CpRuCl(PPh_3)_2$ (0.05 g, 0.068 mmol) in CH_2Cl_2 (5 ml) was added a CH_2Cl_2 (5 ml) solution of $Ph_2PC_6H_4OH$ (0.038 g, 0.068 mmol) and the reaction mixture was stirred at room temperature for 6 h. The resulting solution was evaporated under reduced pressure and the residue was dissolved in diethyl ether (10 ml) and the solution was passed through celite and the filtrate on storing at 0 °C gave orange-red crystalline product. Yield: 78% (0.038 g, 0.054 mmol), m.p.: 168–170 °C (dec.). Anal. Calc. for $C_{41}H_{34}OP_2Ru$: C 69.78; H 4.86. Found: C 69.03; H 4.67%. ^1H NMR ($CDCl_3$): δ 4.10 (s, C_5H_5, 5H), 6.85–7.04 (m, *phenyl*, 4H), 7.11–7.72 (m, P*Ph*, 25H). $^{31}P\{^1H\}$ NMR ($CDCl_3$): δ 44.2 (d, *P* Ph_3, $^2J_{PRuP}$ = 36.4 Hz), 57.4 (d, *P* Ph_2, $^2J_{PRuP}$ = 36.4 Hz). MS (FAB): 706 (M^+ + 1).

5. X-ray crystal structure analysis of 8, 9, 10, 16 and 17

Crystals of compounds **8** and **9** are mounted on Pyrex filaments with epoxy resin. An Enraf-Nonius CAD-4 diffractometer was used for the unit cell determination and intensity data collection. The initially obtained unit cell parameters were refined by accurately centering randomly selected reflections in the 2θ ranges given in Table 1. General procedures for crystal alignment and collection of intensity data on the Enraf-Nonius CAD-4 diffractometer have been published [20]. Periodic monitoring of check reflections showed stability of the intensity data. Details of the crystal and data collection are given in Table 1. The data were corrected for Lorentz and polarization effects [21] and an empirical correction for absorption was applied using ψ scan data from several reflections with χ near 90°. The metal atom positions were obtained from sharpened Patterson functions and the remainder of the structures developed by successive cycles of full-matrix, least-squares refinement followed by calculation of a difference map. Hydrogen atoms were placed in calculated positions (C–H = 0.95 Å) with isotropic displacement parameters 1.2 times those of the attached atom and included as riding contributions. The calculations were performed with the SHELXTL PLUS [22] program package. Crystals of compounds **10, 16, 17** and **18** were mounted in a Cryoloop™ with a drop of Paratone oil and placed in the cold nitrogen stream of the Kryoflex™ attachment of a Bruker APEX CCD diffractometer. A full sphere of data was collected using 606 scans in ω (0.3° per scan) at ϕ = 0, 120 and 240° using the SMART software package [23]. The raw data were reduced to F^2 values using the SAINT+ software [24] and a global refinement of unit cell parameters employing all reflections chosen from the full data set was performed. Multiple measurements of equivalent reflections provided the basis for an empirical absorption correction as well as a correction for any crystal deterioration during the data collection (SADABS [25]). The structure of **10** was solved by direct methods [26] while the position of metal atom was obtained from a sharpened Patterson function for the complexes **16** and **17**. In the latter case, the structure was developed as described for **8** and **9**. Both structures were refined by full-matrix least-squares procedures using the SHELXTL program package [27]. Hydrogen atoms were placed in calculated positions and included as riding contributions with isotropic displacement parameters as described for **8** and **9**.

6. Supporting information available

Full details of data collection and structure refinement have been deposited with the Cambridge Crystallography Data Centre, CCDC nos. 231483, 231484, 231485, 231481 and 231482 for compounds [Mo(CO)$_5$-(PPh$_2$C$_6$H$_4$OCH$_2$OCH$_3$)](**8**), [Mo(CO)$_5${PPh(C$_6$H$_4$OCH$_2$-OCH$_3$)$_2$}] (**9**), [Ru(OC$_6$H$_4$PPh$_2$)$_3$] (**10**) [PdCl (PPh$_2$C$_6$H$_4$-OH)(PPh$_2$C$_6$H$_4$O)] [Ph$_2$P(CH$_2$OCH$_3$)(C$_6$H$_4$OH)Cl] (**16**) and [Pd(PPh$_2$C$_6$H$_4$O)$_2$] (**17**), respectively. Copies of this information may be obtained free of charge from the Director, CCDC, 12 Union Road, Cambridge CB2 1EZ, UK (fax: +44-1223-336033; e-mail: deposit@ccdc.cam.ac.uk or www://http.ccdc.cam.ac.uk).

Acknowledgements

We are grateful to the Department of Science and Technology (DST), Council of Scientific and Industrial Research (CSIR), New Delhi, India for generous support. SP thanks CSIR for JRF and SRF fellowships. We also thank RSIC, Mumbai, Sophisticated Instrumentation Facility (SIF), Bangalore, the Center for Drug Research Institute, Lucknow for spectral data and Louisiana Board of Regents through Grant LEQSF(2002–03)-ENH-TR-67 for purchase of the CCD diffractometer and the Chemistry Department of Tulane University for support of the X-ray laboratory.

References

[1] (a) A. Bader, E. Lindner, Coord. Chem. Rev. 108 (1991) 27;
(b) E. Lindner, E. Glaser, J. Organomet. Chem. 391 (1990) C37.

[2] (a) E. Lindner, U. Schober, R. Fawzi, W. Hiller, U. Englert, P. Wegner, Chem. Ber. 120 (1987) 1621;
(b) T.B. Rauchfuss, F.T. Patino, D.M. Roundhill, Inorg. Chem. 14 (1975) 652.

[3] C. Nachtigal, S. Al-Gharabli, K. Eichele, E. Lindner, H.A. Mayer, Organometallics 21 (2002) 105.

[4] (a) P. Braunstein, D. Matt, D. Nobel, J. Am. Chem. Soc. 110 (1988) 3207;
(b) W. Keim, New J. Chem. 11 (1987) 531.

[5] (a) M.S. Balakrishna, K. Ramaswamy, R.M. Abhyankar, J. Organomet. Chem. 560 (1998) 131;
(b) M.S. Balakrishna, R.M. Abhyankar, J.T. Mague, J. Chem. Soc. Dalton Trans. (1999) 1407;
(c) M.S. Balakrishna, R. Panda, J.T. Mague, Inorg. Chem. 40 (2001) 5620;
(d) M.S. Balakrishna, R.M. Abhyankar, M.G. Walawalker, Tetrahedron Lett. 42 (2001) 2733;
(e) M.S. Balakrishna, M.G. Walawalker, J. Organomet. Chem. 628 (2001) 76;
(f) S. Priya, M.S. Balakrishna, J.T. Mague, Inorg. Chem. Commun. 4 (2001) 437;
(g) S. Priya, M.S. Balakrishna, J.T. Mague, S.M. Mobin, Inorg. Chem. 42 (2003) 1272;
(h) S. Priya, M.S. Balakrishna, J.T. Mague, J. Organomet. Chem. 679 (2003) 116;
(i) S. Priya, M.S. Balakrishna, S.M. Mobin, R. McDonald, J. Organomet. Chem. 688 (2003) 227.

[6] (a) J. Andrieu, J.-M. Camus, J. Dietz, P. Richard, R. Poli, Inorg. Chem. 40 (2001) 1597;
(b) K. Neplechova, J. Kasparkova, O. Vrana, O. Novakova, A. Habtemarium, B. Watchman, P.J. Sadler, V. Brabec, Mol. Pharmacol. 56 (1999) 20;
(c) N. Margiotta, A. Habtemarium, P.J. Sadler, Angew Chem. Int. Ed. Engl. 36 (1997) 1185;
(d) A. Habtemariam, J.A. Parkinson, N. Margiotta, T.W. Hambley, S. Parsons, P.J. Sadler, J Chem. Soc. Dalton Trans. (2001) 362;
(e) A.D. Burrows, M.F. Mahon, M.T. Palmer, J Chem. Soc. Dalton Trans. (2000) 1669;
(f) E. Lindner, J. Wald, K. Eichele, R. Fawzi, J. Organomet. Chem. 601 (2000) 220.

[7] (a) T.B. Rauchfuss, Inorg. Chem. 16 (1977) 2966;
(b) H. Luo, I. Setyawati, S.J. Rettig, C. Orvig, Inorg. Chem. 34 (1995) 2287.

[8] Y. Yamamoto, R. Sato, M. Ohshima, F. Matsuo, C. Sudoh, J. Organomet. Chem. 489 (1995) C68.

[9] J.-F. Ma, Y. Kojima, Y. Yamamoto, J. Organomet. Chem. 616 (2000) 149.

[10] (a) C. Bolzati, F. Tisato, F. Refosco, G. Bandoli, A. Dolmella, Inorg. Chem. 35 (1996) 16221;
(b) A.M. Trzeciak, J.J. Ziolkowski, T. Lis, R. Choukroun, J. Organomet. Chem. 575 (1999) 87;
(c) M. Canestrari, B. Chaudret, F. Dahan, Y.-S. Huang, R. Poilblanc, T. Chong, J Chem. Soc. Dalton Trans. (1990) 1179.

[11] L. Miguel, M. Basso-Bert, R. Choukroun, R. Madhouni, B. Eichhorn, M. Sanchez, M.R. Mazieres, J. Jaud, J. Organomet. Chem. 490 (1995) 21.

[12] C.E. Jones, B.L. Shaw, B.L. Turtle, J. Chem. Soc. Dalton Trans. (1974) 992.

[13] R.B. King, Inorg. Chem. 2 (1963) 936.

[14] M.A. Bennett, L. Pratt, G. Wilkinson, J. Chem. Soc. (1961) 2037.

[15] D.J. Darensbourg, R.L. Kump, Inorg. Chem. 17 (1978) 2680.

[16] D. Drew, J.R. Doyle, Inorg. Synth. 13 (1972) 48.

[17] D.A. White, Inorg. Synth. 13 (1972) 52.

[18] J.A. McCleverty, G. Wilkinson, Inorg. Synth. 8 (1966) 211.

[19] J. Chatt, L.M. Venanzi, J. Chem. Soc. (1957) 4735.

[20] J.T. Mague, C.L. Lloyd, Organometallics 7 (1988) 983.

[21] K. Harms, S. Wocadlo, Program to Extract Intensity Data from Enraf-Nonius CAD-4 Files: University of Margburg, 1987.

[22] Bruker-AXS, SHELXTL PLUS version 5.1: Madison, WI, 1995.

[23] Bruker-AMX SMART version 5.625: Madison, WI, 2000.

[24] Bruker-AXS SAINT+ version 6.35A: Madison, WI, 2002.

[25] G.M. Sheldrick, SADABS Version 2.05, University of Göttingen, Germany, 2002.

[26] G.M. Sheldrick, SHELXS97 and SHELXL97, University of Göttingen, Germany, 1997.

[27] Bruker-AXS SHELXTL Version 6.1: Madison, WI, 2000.